



UWS Academic Portal

The impact of gaseous ozone penetration on the disinfection efficiency of textile materials

Epelle, Emmanuel I.; Macfarlane, Andrew; Cusack, Michael; Burns, Anthony; Amaeze, Ngozi; Mackay, William; Yaseen, Mohammed

Published in:
Ozone: Science & Engineering

DOI:
[10.1080/01919512.2022.2066503](https://doi.org/10.1080/01919512.2022.2066503)

E-pub ahead of print: 26/04/2022

Document Version
Publisher's PDF, also known as Version of record

[Link to publication on the UWS Academic Portal](#)

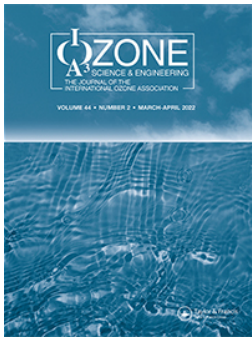
Citation for published version (APA):
Epelle, E. I., Macfarlane, A., Cusack, M., Burns, A., Amaeze, N., Mackay, W., & Yaseen, M. (2022). The impact of gaseous ozone penetration on the disinfection efficiency of textile materials. *Ozone: Science & Engineering*, 1-15. [BOSE A 2066503]. <https://doi.org/10.1080/01919512.2022.2066503>

General rights

Copyright and moral rights for the publications made accessible in the UWS Academic Portal are retained by the authors and/or other copyright owners and it is a condition of accessing publications that users recognise and abide by the legal requirements associated with these rights.

Take down policy

If you believe that this document breaches copyright please contact pure@uws.ac.uk providing details, and we will remove access to the work immediately and investigate your claim.



The Impact of Gaseous Ozone Penetration on the Disinfection Efficiency of Textile Materials

Emmanuel I. Epelle, Andrew Macfarlane, Michael Cusack, Anthony Burns, Ngozi Amaeze, William Mackay & Mohammed Yaseen

To cite this article: Emmanuel I. Epelle, Andrew Macfarlane, Michael Cusack, Anthony Burns, Ngozi Amaeze, William Mackay & Mohammed Yaseen (2022): The Impact of Gaseous Ozone Penetration on the Disinfection Efficiency of Textile Materials, *Ozone: Science & Engineering*, DOI: [10.1080/01919512.2022.2066503](https://doi.org/10.1080/01919512.2022.2066503)

To link to this article: <https://doi.org/10.1080/01919512.2022.2066503>



© 2022 The Author(s). Published with license by Taylor & Francis Group, LLC.



Published online: 26 Apr 2022.



Submit your article to this journal [↗](#)



Article views: 67



View related articles [↗](#)



View Crossmark data [↗](#)

The Impact of Gaseous Ozone Penetration on the Disinfection Efficiency of Textile Materials

Emmanuel I. Epelle^{a,b}, Andrew Macfarlane^b, Michael Cusack^b, Anthony Burns^b, Ngozi Amaeze^c, William Mackay^c, and Mohammed Yaseen^a

^aSchool of Computing, Engineering & Physical Sciences, University of the West of Scotland, Paisley, PA1 2BE, UK; ^bACS Clothing, ML1 4GP, UK; ^cSchool of Health & Life Sciences, University of the West of Scotland, Paisley, PA1 2BE, UK

ABSTRACT

The utilization of gaseous ozone (a powerful oxidant) in air, for disinfection and sterilization purposes, has been extensively studied for diverse applications; however, the optimal deployment of this technology for textile disinfection is deserving of further research attention and is this the focus of this work. In this study, the penetration efficiency of ozone gas into hard-to-reach regions of different garment types is critically examined. The impacts of garment packing density, hanging orientation and ozonation duration are also considered, and the resultant disinfection efficiencies are comparatively analyzed. An ozonation chamber fitted with remote ozone detection is utilized for the ozonation of fabric swatches inoculated with *Escherichia coli* bacteria. The number of colony-forming units per cm² and the bacterial lawn area fraction are evaluated pre- and post-ozonation to quantify the level of disinfection. This study shows that the attainment of sufficient ozone concentrations in hard-to-reach regions of different garment types coupled with the inter-garment spacing utilized are vital for effective decontamination. This study also demonstrates the effectiveness of ozonation as a necessary technology for decontamination, particularly in this era, where the sterilization of textiles and other materials is paramount for public health and safety.

ARTICLE HISTORY

Received 23 December 2021
Accepted 12 April 2022



KEYWORDS

Disinfection; Garment packing; Microbial decontamination; Ozone concentration; Penetration

Introduction

Ozone (O₃) is a potent antimicrobial agent with numerous applications in several industries such as healthcare (Rogers 2012; Karim et al. 2020), food (Kim, Yousef, Dave 1999; Guzel-Seydim, Greene, Seydim 2004; Rosenblum, Ge, Bohrerova, Yousef, Lee 2012), wastewater treatment (Malik, Ghosh, Vaidya, Mudliar 2020; Rekhate and Srivastava, 2020) and aquaculture (Summerfelt, Sharrer, Tsukuda, Gearheart 2009; Sharrer and Summerfelt, 2007; Gonçalves and Gagnon, 2011). Its rapid reactivity, penetrability and spontaneous decomposition into oxygen make it an important disinfectant as far as microbiological safety is concerned. Besides its disinfection capabilities, ozone's multifunctionality as a decolorizer and a deodorizer has made it particularly useful for water purification and the eradication of unpleasant odors in garment treatment. Furthermore, hybrid techniques, utilizing ultraviolet irradiation (Summerfelt 2003; Szeto, 2020), chlorination (Dosti, Guzel-Seydim, Greene 2005) and other oxidative chemicals have shown increased disinfection tendencies when combined with ozone.

Of the numerous published works, which have repeatedly demonstrated the disinfection efficacy of ozone (Kowalski, Bahnfleth, Striebig, Whittam 2003; Guzel-Seydim, Greene, Seydim 2004; Lage Filho 2010; Martinelli, Giovannangeli, Rotunno, Trombetta, Montomoli 2017; Wang, Quan, Chen, Yu, Liu 2019), an insignificant fraction of these has focused on airborne garment disinfection in the textile processing industry. The main application of ozone within this industry at present is as a bleaching agent to remove color from fabric. Primarily, this process involves the introduction of ozone in high concentrations to garments, which enhances the dye's permeance to intensities that are no longer visible on the surface of the material (Sevimli and Sarikaya, 2002; Körlü 2018). According to these studies, prolonged exposure to ozone enhances its penetration into the fabric substrates, and this further enhances the bleaching process. Ozone is also used in wash cycles in some laundry companies in the UK. Rice et al. (2010) presented a comprehensive review of successful deployments of ozone laundry systems in several establishments. Their review mentions cost

CONTACT Mohammed Yaseen  mohammed.yaseen@uws.ac.uk  School of Computing, Engineering & Physical Sciences, University of the West of Scotland, Paisley, PA1 2BE, United Kingdom

© 2022 The Author(s). Published with license by Taylor & Francis Group, LLC.

This is an Open Access article distributed under the terms of the Creative Commons Attribution-NonCommercial-NoDerivatives License (<http://creativecommons.org/licenses/by-nc-nd/4.0/>), which permits non-commercial re-use, distribution, and reproduction in any medium, provided the original work is properly cited, and is not altered, transformed, or built upon in any way.

savings (via reduced energy consumption via cold washes) as high as 81% per year. From an environmental perspective, the use of ozone in laundry systems significantly decreases the need for chemicals that end up in laundry wastewaters (Rice et al., 2009; Neral 2018). Furthermore, the presence of ozone in laundry systems increases dissolved oxygen levels; thus, facilitating the biodegradability of discharged pollutants into carbon dioxide and water.

Despite these advancements, little is understood concerning the penetrability of ozone gas in garments with different morphological structures and the resulting impact on the disinfection efficiency attainable. The interdependence between ozonation duration, ozone concentration, temperature, fabric morphology, and fabric packing density remains unclear. The pockets and other hard-to-reach regions of a garment constrain the attainable levels of microbial destruction. This has not been adequately studied/quantified in previous contributions. This paper addresses these knowledge gaps by analyzing gaseous ozone's penetration and disinfection potencies under different processing conditions. This knowledge is of particular importance in these unprecedented times of the COVID-19 pandemic, with ozone showing potent disinfection power against the SARS-COV-2 virus (Dennis, Cashion, Emanuel, Hubbard 2020; Rubio-Romero, Del Carmen Pardo-ferreira, Torrecilla-García, Calero-Castro 2020; Valdenassi

et al. 2020; Manjunath, Sakar, Katapadi, Balakrishna 2021). We expect the presented findings to better inform commercial users of ozone technology and manufacturers of airborne ozone equipment about the factors influencing the efficiency of their processes.

Methodology

The ozone cabinet employed in this study (Figure 1) utilizes a computerized double-stage operating cycle, which can be safely operated by an external Human Machine Interface (HMI) touch screen. The air-tight chamber was situated in an enclosed room equipped with adequate ventilation systems to further mitigate ozone exposure. Both ozone generation and destruction occur within a single-timed cycle, allowing the attainment of low ozone concentrations upon completion of the cycle. Table 1 summarizes the key parameters of the unit. To operate the ozone cabinet, the garments of interest were placed on the hanging rail (Figure 1(b)), after which the chamber was shut. The desired ozone exposure duration was applied via the HMI (located on the chamber's door) to commence the treatment cycle. Upon completion (as determined by the sensor readings), the chamber was opened and concentration/penetration profiles analyzed. Assessments of the disinfection efficiency also followed after the treatments.

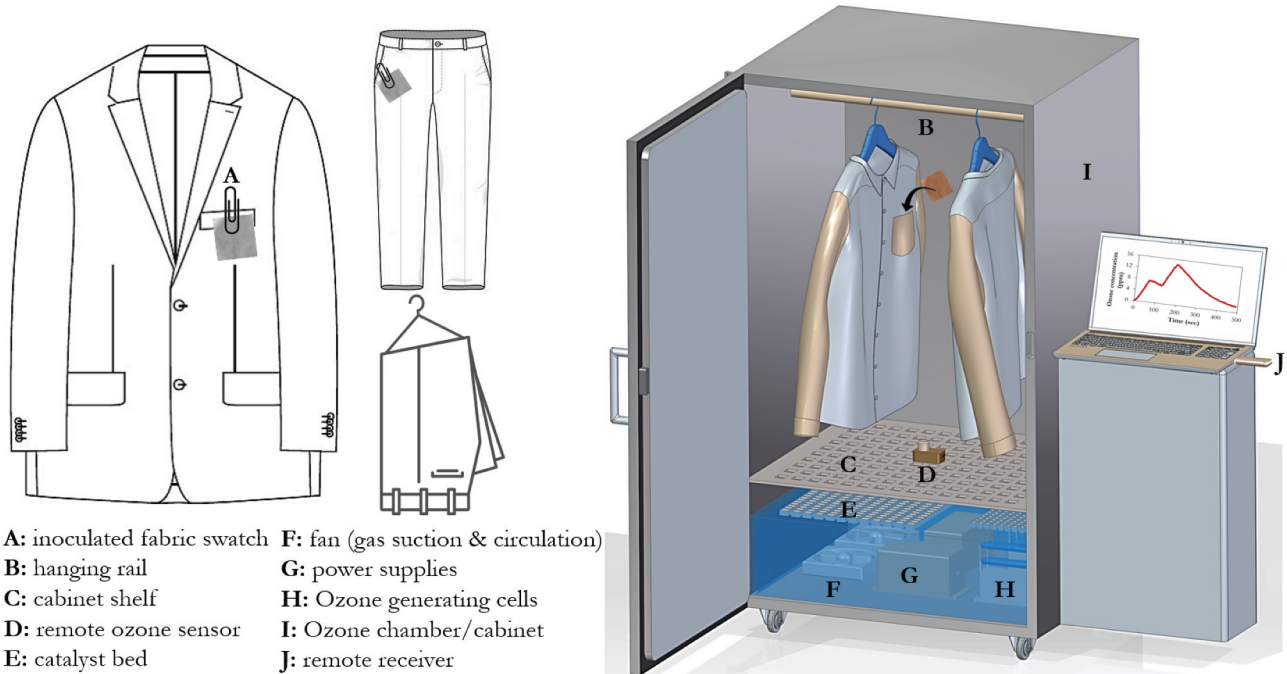


Figure 1. Ozone chamber utilized for penetration and disinfection analysis, showing the internal components, the different garment types and the respective orientations employed.

Table 1. Parameters of the ozone cabinet.

Parameter	Value
Volume	1.26 m ³
Input voltage	230 V, 50 Hz
Air flow rate	450 m ³ .hr ⁻¹ (generation); 850 m ³ .hr ⁻¹ (destruction)
Ozone cycle time	4, 8, 16, 32 mins
Ozone output	10 g.hr ⁻¹ (via dielectric barrier discharge)
Operating conditions	Temperature (-5 °C to 40 °C); Relative humidity (95% max.)
Decomposition mechanism	Catalytic decomposition via internal recirculation through a porous activated carbon bed.

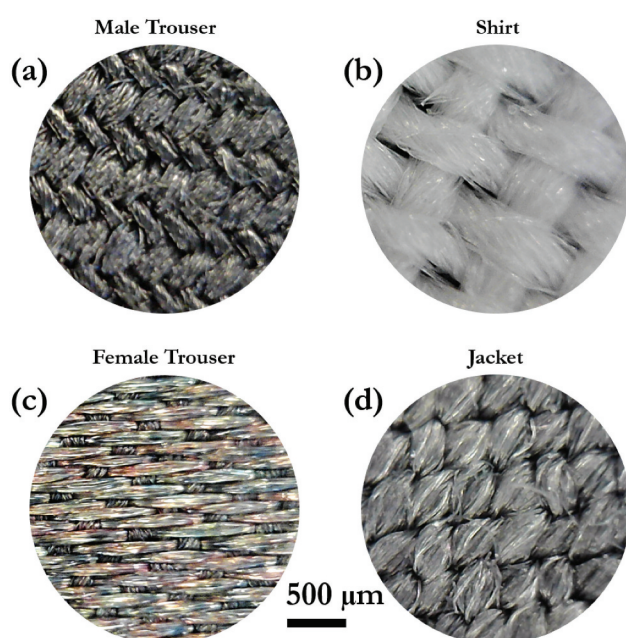


Figure 2. Micrographic images of the garments' weave structure (images were obtained using an optical microscope). Compared to the other textile materials, the shirt (c) can be seen to have increased porosity between the fibers, thus favoring ozone penetration.

Penetration

To analyze ozone penetration, a calibrated sensor (Shanghai JSR Industries, China) small enough to be accommodated in a pocket and capable of real-time remote data transfer was employed. The sensor (0–100 ppm measuring range) shown in Figure 1(d), utilizes Bluetooth signals for data transfer to the receiver connected to a computer external to the cabinet. Thus, ozone concentrations during multiple cycles can be

analyzed at several locations of interest and for different garment types. 4 garment types (jackets, male trousers, female trousers and a shirt) were used in this study. The sensor was placed in the inner jacket pocket, outer shirt pocket, front trouser pockets, and in the open for comparative assessments of ozone concentration. There is considerable proximity between these chosen test locations and regions of a garment susceptible to the transfer and storage of body fluids (the armpit and groin area).

Thus, the penetration level of ozone into these hard-to-reach areas inevitably indicates the attainable disinfection level in these regions which are relatively prone to contamination.

Fabric morphology

Figure 2 and Table 2 show the morphological structures and properties of the respective garments explored in this study. All 4 garments possess different fiber arrangements; in particular, the female trouser shows a tightly packed structure. We demonstrate in the latter sections of this paper, the relationship between the fiber packing density and the extent of ozone penetration. As shown in Table 2 and Figure 1 two hanging orientations are also explored in relation to their levels of ozone penetration.

Preparation of test organism and fabric swatches

A representative colony of the test organism was transferred into 10 mL of Luria broth (Sigma Aldrich, St Louis, USA) and incubated at 37 °C at 150 rpm for 24 h. From the overnight culture, 1 mL of bacterial suspension was transferred into a sterile 1.5 mL Eppendorf tube and centrifuged at 10,000 rpm for 5 min in a microcentrifuge. The harvested cells were washed twice with phosphate buffer saline (PBS), and the absorbance (at 570 nm) of each bacterial suspension was adjusted to an optical density of 0.2 (± 0.02), corresponding to 10⁹ *E.coli* bacteria/mL. Fabric swatches (6.5 cm by 6.5 cm) were prepared from the shirt material and sterilized in 70% ethanol solution. Using an Eppendorf pipette, the swatches were inoculated at their centers, on a non-absorbent sterile surface with 80 μ L aliquots of the prepared bacteria

Table 2. Garment properties, with material composition as obtained from manufacturers.

Garment	Mass (kg)	Material type and composition	Folding
Jacket	0.55	53% Polyester; 43% Wool; 4% Linen (inner jacket lining)	Not folded
Male trouser	0.40	50% Polyester; 50% Wool	Folded and not folded (see Figure 1)
Female trouser	0.20	97% Polyester; 3% Elastane	Not folded
Shirt	0.20	65% Polyester; 35% cotton	Not folded

suspension (yielding 8×10^7 cells). The volume of suspension applied was sufficient to allow full coverage of the swatches' surface area.

Disinfection

Before disinfecting the fabric swatches, the garments to be used in this study were autoclaved to ensure sterility. Using sterile forceps and paperclips, the inoculated fabric swatches were transferred and attached to the desired garment for ozonation. Dip slides (Dip-Slides, UK), with a thick nutrient agar layer, were applied for surface testing in this study. The slides were placed onto the desired surface (pre- and post-ozonation) with gentle pressure applied for 10 sec. These were subsequently incubated at 37 °C for 24 hours. Inoculated swatches (without ozone treatment) were also tested using the dip slides; this served as the control experiment. The slides contain a red spot dye – 2,3,5-triphenyl tetrazolium chloride (TTC), which allows the enumeration of microbial colonies in solid structure media. Although this dye is colorless in an oxidized form, it turns red due to enzymatic reduction by microorganisms—generating formazan in the process (Beloti et al. 1999). After incubation, the number of red spots is counted using an image processing software (MATLAB® 2020b), to enumerate the percentage bacteria removal.

Analysis of initial bacterial concentration

Before carrying out disinfection experiments with ozone, it was desired to establish a baseline of the contamination level on fabric swatches, while also examining the performance of the dip slides used; these slides were tested on the fabric and in water. Figure 3 shows that for volumes above 10 μL of bacteria suspension, lawns of bacteria cells are formed on the slide, thus implying that counting the number of red colonies is insufficient for a robust evaluation of disinfection level. These lawns can be seen as a cloudy/faint appearance on the agar, whereas the agar slide infected with 10 μL of bacteria suspension, has a much clearer appearance. Thus, approximate analyses of the lawn area fraction had to be performed. This is particularly important since the fabric swatches utilized in this study were inoculated with 80 μL of bacteria suspension. This volume was sufficient to cover the swatch (6.5 cm by 6.5 cm), which was, in turn, able to accommodate the full area of the dip slide (5 cm by 2 cm). We examine the disinfection level attained by evaluating the reduction in the lawn area fraction and the number of colony-forming units (CFU) – the bacterial concentration. These are carried out with advanced image processing algorithms in MATLAB® R2020b. The bacterial concentration per cm^2 of the dip slide agar area (10 cm^2) is calculated according to Eq. 1; where the corrected pick-up rate (CPUR) = 2 (approximately, 50% of bacteria is picked up from a surface).

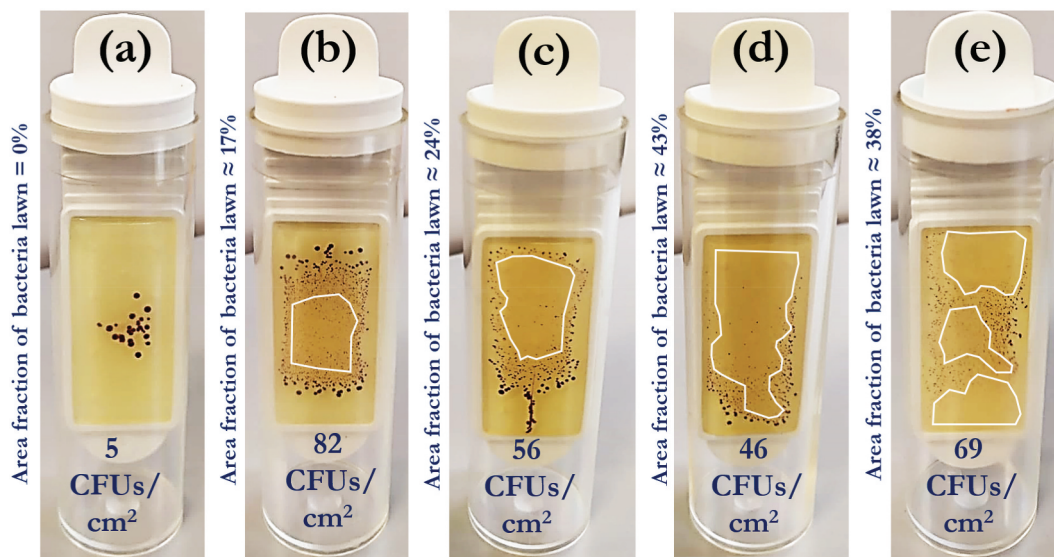


Figure 3. Obtained bacterial concentrations at different volumes of utilized bacterial suspension (a) 10 μL (b) 25 μL (c) 40 μL (d) 65 μL (e) 80 μL . These volumes of bacteria suspension are applied directly to different fabric swatches after which the dip slides are used to pick up viable cells. Upon incubation, a lawn of bacterial colonies (represented by the area fraction) is observed; this area fraction increases with the applied volume of the bacterial suspension.

$$CFUs/cm^2 = \frac{\text{Number of colonies} \times CPUR}{\text{Agar area}} \quad [1]$$

Assessment of bacteria-fiber interaction using Scanning Electron Microscopy (SEM)

To prepare samples for SEM, 100 μL of the bacteria suspension (Section 2.3) was added to a 10 mm by 10 mm fabric swatch and incubated in a 6-well plate at 37°C for 24 hours. The sample was then washed with PBS (0.01 M) and subsequently fixed with a solution of 2% paraformaldehyde, 2.5% glutaraldehyde and 0.1 M phosphate buffer (pH 7.4) for at least 30 min at room temperature. The fixed samples were dehydrated in gradually increasing concentrations of ethanol solutions (50, 70, 80, 90, 95 and 99% v/v). The specimens were subsequently treated with tert-Butanol, and then freeze-dried (Christ Alpha 1–2 LD plus). This was followed by gold sputter coating (Emscope SC500), after which the samples were mounted on aluminum stubs using a double-sided carbon tape and thereafter, imaged (Hitachi S-4100).

Results and discussion

Optimizing the chamber's performance

To better understand the performance of the unit, and the required duration for reproducibility of multiple treatment cycles, consecutive cycles were run after different waiting timeframes. Figure 4 shows the profiles for both closed and open conditions; the sensor was placed on the cabinet shelf, and no garment was placed in the chamber. Under the closed condition, the first cycle was run to ensure sterility of the chamber; this also ensured that the required warmup time was met for optimal performance of the ozone generating cells. Once this cycle was completed, the doors of the chamber

were left shut, and another cycle was run immediately. The profile for this cycle served as the baseline to compare subsequent runs. After this cycle, there was a waiting time of 1 minute before another cycle was run; Figure 4(a) shows the profiles for waiting durations of 3, 5, 7 and 9 mins; the chamber remained closed during these successive runs. It can be observed that the curves begin to merge after the *Baseline* curve, with a final peak of 17 ppm.

A similar procedure was repeated with the open scenario; however, the door of the chamber was opened for 1, 3, 5, 7, and 9 mins respectively before running the ozonation cycle. This allowed a fresh air supply into the chamber for each run. Compared to the closed scenario, a final peak of 15 ppm was attained. This is attributable to the fresh air supply at each interval, which flushed out the chamber of residual ozone and oxygen radicals. It is also worth mentioning that the chamber was opened and closed instantaneously after it was sanitized, to generate the *Baseline* curve of Figure 4(b). It is observed that this curve is very similar to those of 1, 3, 5, 7 and 9 min; whereas there is a considerable difference between the *Sanitize* and *Baseline* curves for the closed scenario. Since the chamber needs to be opened to put in new garments (for subsequent tests presented), a waiting time of 3 mins was maintained, between successive runs to establish the same ozonation conditions for all tests performed in the study.

The double-peaked profile of the ozone generation curves is a result of the default ozone control system implemented in the chamber by the manufacturers. After the ozone generators are started, they momentarily turn off after a minute of operation, and automatically restart again, until the 3rd minute, after which the main ozone decomposition cycle begins. This pre-programmed sequence provides little flexibility compared to the apparatus utilized in (Epelle et al. 2022b), where the desired ozone concentration can be

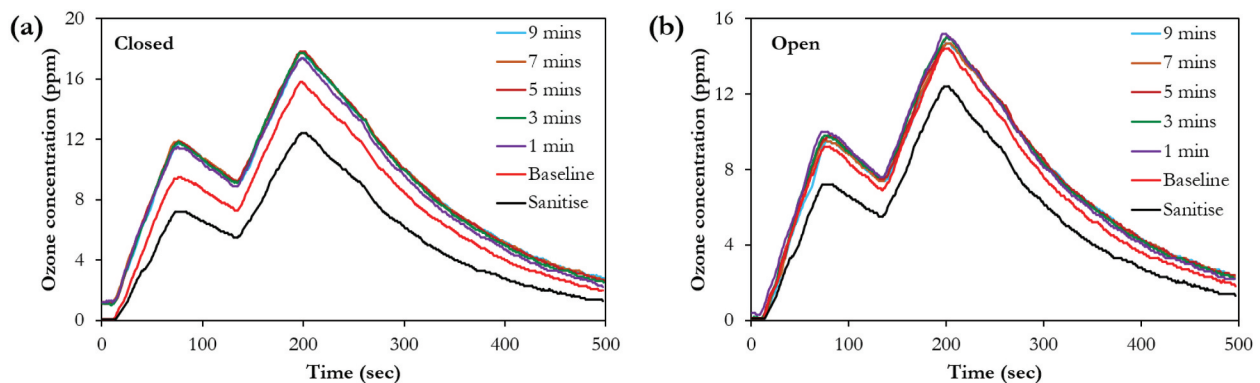


Figure 4. Reproducibility test for closed and open conditions of the ozone chamber, where the *Baseline* curve represents time, $t = 0$ min.

maintained for the required duration. For a chamber volume of 1.26 m^3 , and an ozone-generating capacity of 10 g/hr , the theoretically-computed concentration in $\sim 80 \text{ s}$, is expected to be $\sim 89 \text{ ppm}$. However, Figure 4(b) and 5(a) (the typical cycle profiles utilized herein) reveal a concentration of only 10 ppm . This can be attributed to the convention of reporting the generating capacity, on the basis of a pure oxygen feed to the equipment, among many manufacturers of ozone-generating equipment. Since air ($\sim 21\%$ oxygen) was used as the feed gas in our experiments, the expected concentration would be significantly lower than in a pure oxygen-feed scenario. The inherent mechanical/electrical inefficiencies of the equipment may have further contributed to the observed 10 ppm concentration attained in approximately 80 s of ozone generation; hence the need for real-time monitoring of the concentration in the ozone chamber.

Figure 5b shows the profile of temperature for a typical cycle (Figure 5(a)). We aimed to observe the impact of ozonation on the ambient conditions in the chamber relative to the initial scenario without ozone. It can be observed that the temperature generally increases compared to the initial condition; a consequence of the heating effect of the ozone generating cells (via dielectric barrier discharge) and the partial pressure of the generated gas (Figure 5(b)). The slight ambient temperature increase signifies minimal impact on ozone stability in the chamber, compared to scenarios where larger temperature changes can negatively affect ozone stability as demonstrated by (Epelle et al. 2022a). For the typical ozonation cycle shown in Figure 5(a), the average relative humidity in the chamber was 38% .

Since the actual amount of ozone produced and sustained in the chamber is significantly affected by factors, such as temperature, humidity, air circulation level, feed gas utilized (air), and contamination level, it was also

important to ascertain ozone's natural decomposition (ND) kinetics in comparison to its decomposition using the activated carbon catalyst. It is worth mentioning that, in the ozone destruction phase, the suction pressure is created, pulling the gas toward the porous catalyst bed in the lower section of the chamber (Figure 1). As shown in Figure 6, the application of a catalyst results in a decomposition rate roughly 24 times that without a catalyst. While this is desirable with regards to lowering the concentration levels rapidly in a single cycle, prolonged contact time, at high concentrations, which is necessary for adequate disinfection may be undermined. Figure 6 also demonstrates that the decomposition of ozone in air follows first-order kinetics. This is in agreement with the works of Li (1998) and Batakiev et al. (2014). In the rest of the results presented in this work, the ozonation cycles were operated with catalytic decomposition.

Ozone penetration and disinfection – single garments

Figure 7 comparatively illustrates the difference between the concentration of ozone gas in the open (sensor on cabinet shelf) and when placed in the pockets of the different garments considered. As expected, the gas concentration in the pockets is lower than that in the open. With the jacket and shirt (Figure 7(a-d)), the double peak signature in the open area is retained. However, there is a far more significant drop in the final peak, with the jackets than the shirt. This is because the sensor was placed in the inner jacket pocket, thus causing a huge penetration barrier for the gas. The placement of the sensor in the shirt's only pocket (which is exterior) and its highly porous weave structure (Figure 2(b)) are the likely reasons for this increased penetration observed in Figure 7(d).

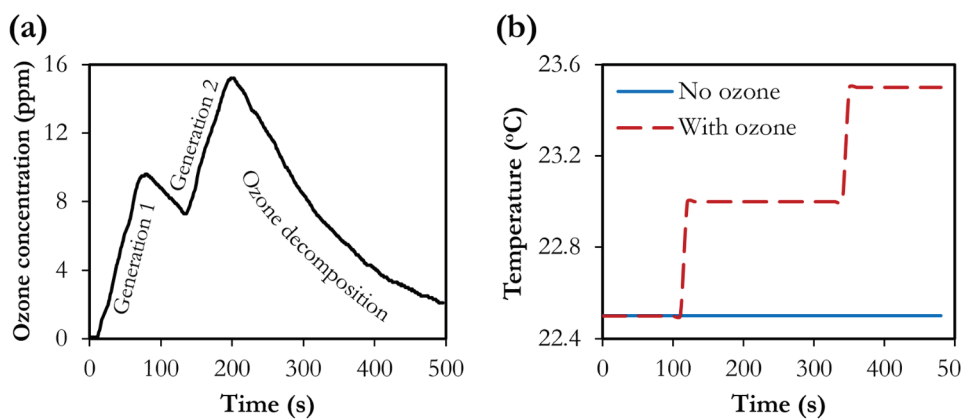


Figure 5. Profiles of process conditions for a typical 8-min cycle. The figure shows the influence of ozone generation on the ambient temperature, in an 8 min ozonation cycle in comparison to a scenario, where no ozone is generated.

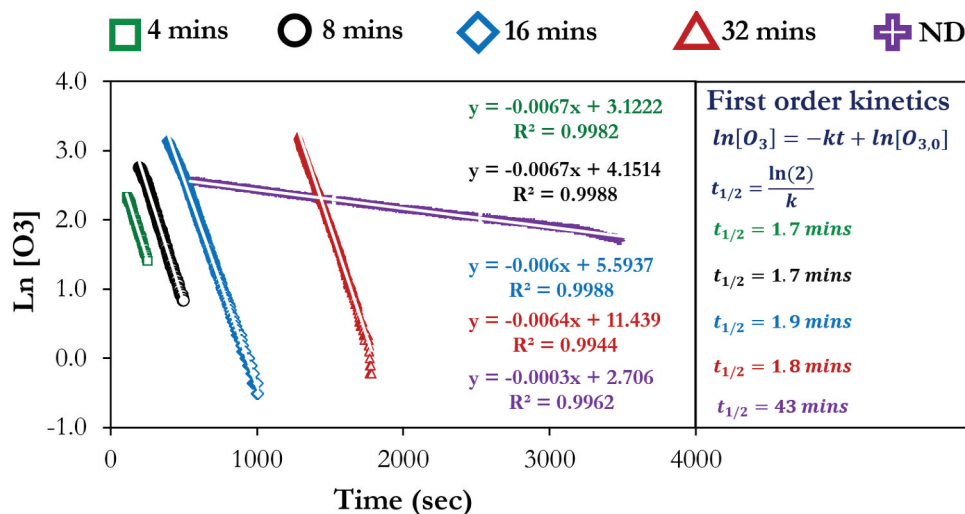


Figure 6. Kinetics of ozone decomposition (for the 4-, 8-, 16-, and 32-min cycles, with the catalyst) and natural decomposition (ND, without the catalyst). For all exposure durations involving the catalyst, the half-life is 1.8 min (± 0.1 min), whereas the ozone half-life without the catalyst is approximately 24 times greater. The average chamber temperature was 20 °C.

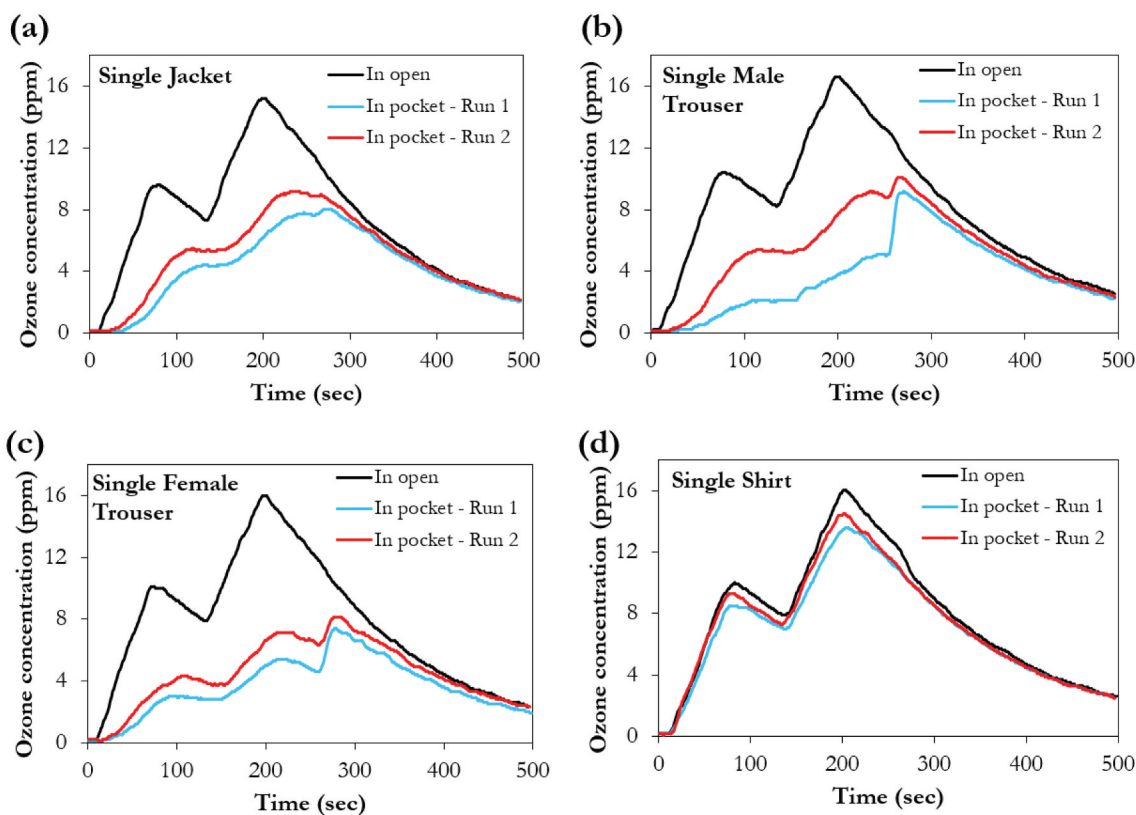


Figure 7. Penetration of ozone into pockets – single-garment tests. Trousers were folded as shown in Figure 1 and the sensor was placed in the inner jacket pocket.

The female and male trousers display a characteristic third peak in the concentration profiles (Figure 7(b-c)). This is attributable to the folded form (Figure 1), employed when hanging the trousers in the chamber. This increases the number of layers/barriers which must be overcome by the gas before it is picked up by the sensor. The response

time of the sensor is < 20 s; hence, the lag in concentration (relative to the *in-open* scenario) is mainly a consequence of the delayed entry of the dense ozone gas (1.8 times the density of air). Despite its lower weight (Table 2), the tightened weave structure of the female trousers as shown in Figure 2(c) has also resulted in the lowest peak

concentration relative to other garments, when the sensor is placed in its pockets (Figure 7(c)). It can also be observed that the second run, (with the sensor in the pockets) repeatedly shows a higher concentration than the first run. This may be attributed to the air circulation in the chamber. Before the first run (Run 1), the garments were in a pressed and compact form; whereas the strong air currents loosened the garments significantly so that better penetration was attained in Run 2.

Similar to the analysis performed in the penetration study, the extent of disinfection attainable when an inoculated swatch is placed on/in the garment pocket is also evaluated (Figure 8). The impact of the resultant penetration efficiency on the disinfection efficacy is analyzed using the jacket and male trousers only, particularly because of their pronounced fabric thickness relative to the shirt and female trousers. Compared to Figure 3(e) (the control), there is a significant removal of the bacterial lawns after ozonating for 8 mins. Relative to the in-pocket scenario (Figure 8(a)), the bacterial concentration is also massively reduced (by 89%; i.e., from 100 to 11.5 CFUs/cm² Figure 8(b)) when the swatch is placed outside the fabric pocket for more ozone exposure (Figure 8(a)). This level of disinfection is noticeable with both runs (R1 and R2).

Figure 9 shows a similar observation for the trousers (folded) as with the jackets. In this case, 84% bacterial removal was attained (percentage difference between *In*

and *Out*), and no bacterial lawn formation was observed. However, the bacterial concentration observed with the trousers was approximately half of those observed with the jackets (Figures 10(b) and 11(b)). This may be attributed to the thickness & weight (Table 2) of the jacket material and the difficulty of disinfection in such environments compared to the thinner and lighter trousers.

Ozone penetration and disinfection – multiple garments

As ozone chambers in the industry are hardly operated with a single garment in them, it becomes necessary to evaluate the penetration efficiency in a multiple-garment scenario. Figure 10 illustrates the ozone concentration profiles under this condition. We investigated the penetration level when 3 and 5 garments (jackets and male trousers only) are ozonated, under evenly spaced and densely packed conditions. In all cases, the sensor was placed in the inner pocket of the middle garment.

As shown in Figure 10, the spacious configuration always yields better ozone penetration as illustrated by the higher ozone concentrations. Similarly, ozone penetration is better with fewer garments in the cabinet. Compared to Figure 7 (with single garments), there is also a more significant lag time before ozone is first picked up by the sensor (Figure 10). The lag time increases when the packing is changed from spacious

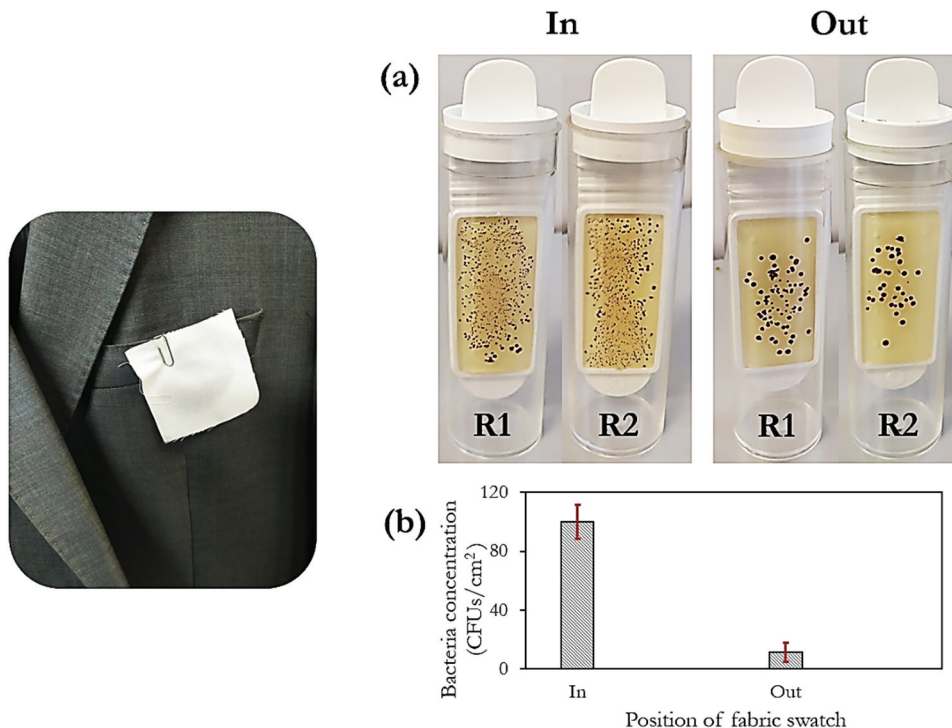


Figure 8. Disinfecting a fabric swatch attached to 1 jacket. The swatch was placed on the outer pocket (*Out*) and in the inner pocket (*In*), as with the penetration study. Qualitative (a) and quantitative (b) comparisons are shown for the in and out scenarios, respectively.

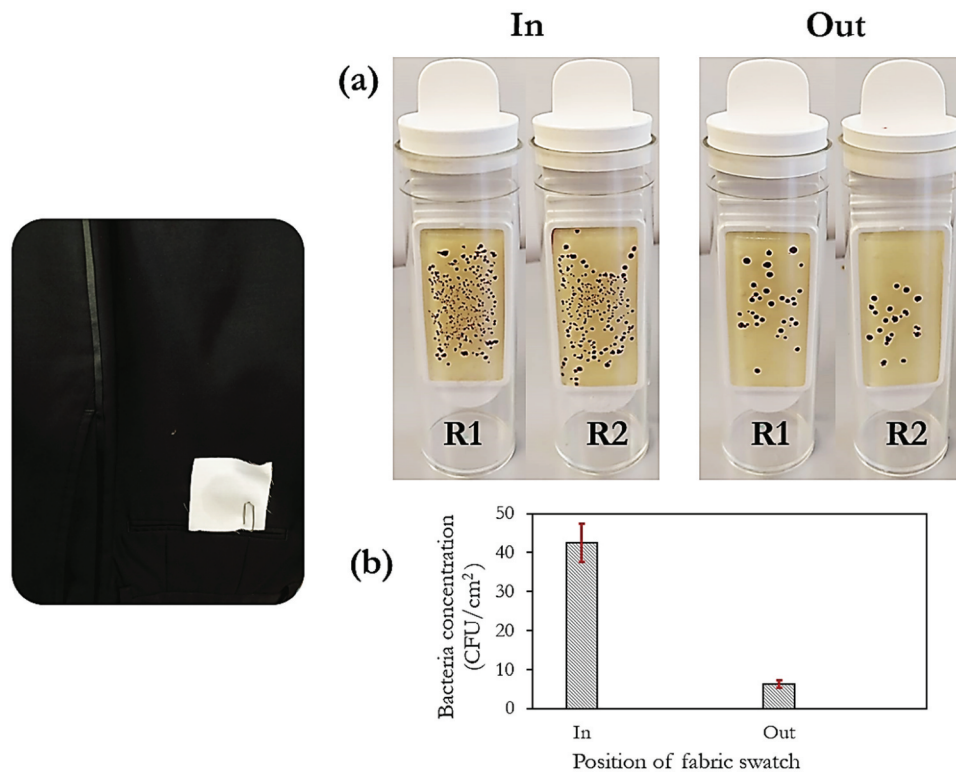


Figure 9. Disinfecting a fabric swatch attached to 1 trouser. The swatch was placed on the outer pocket (*Out*) and in the inner pocket (*In*), as with the penetration study. Qualitative (a) and quantitative (b) comparisons are shown for the in and out scenarios, respectively.

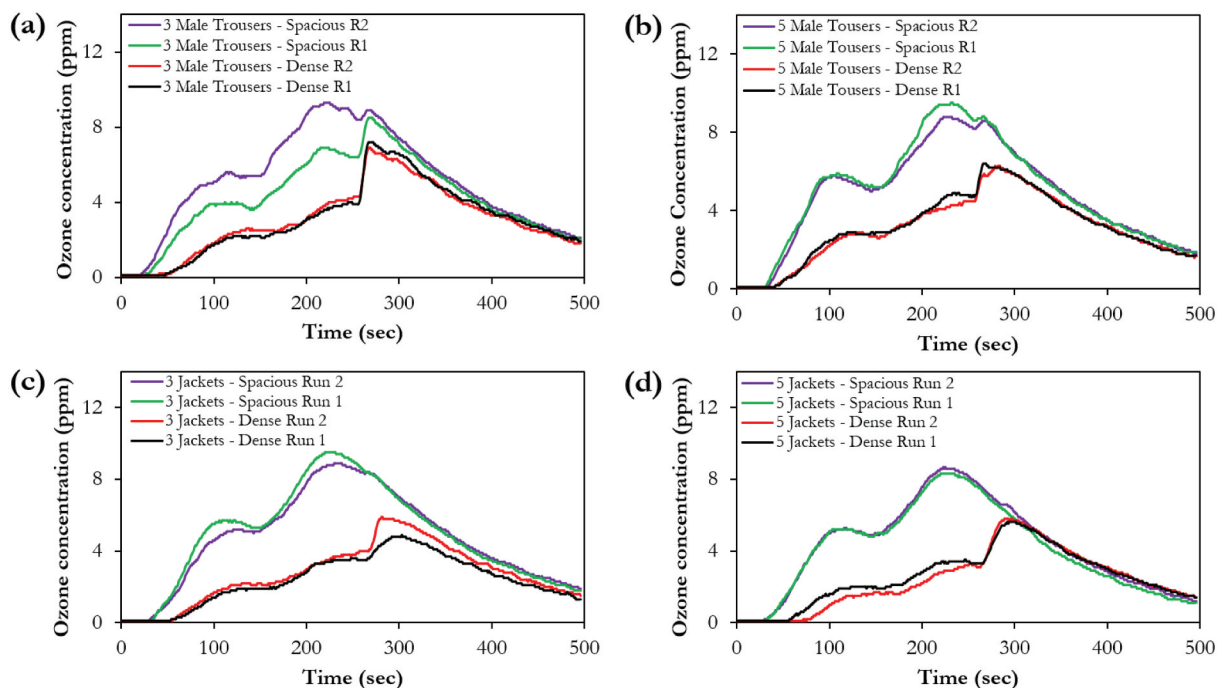


Figure 10. Penetration of ozone into pockets – multiple-garment tests. Trousers were folded as shown in Figure 1 and the sensor was placed in the inner pockets of the middle garments.

to dense. For example, Figure 7(a) shows that 27 sec is required before, ozone is picked up by the sensor when the trousers are spaced, whereas it takes 47 sec under

a densely packed condition, for the same set of 3 trousers. The 3rd peak, which was only noticed with the trousers in the single-garment tests (Figure 7) appeared

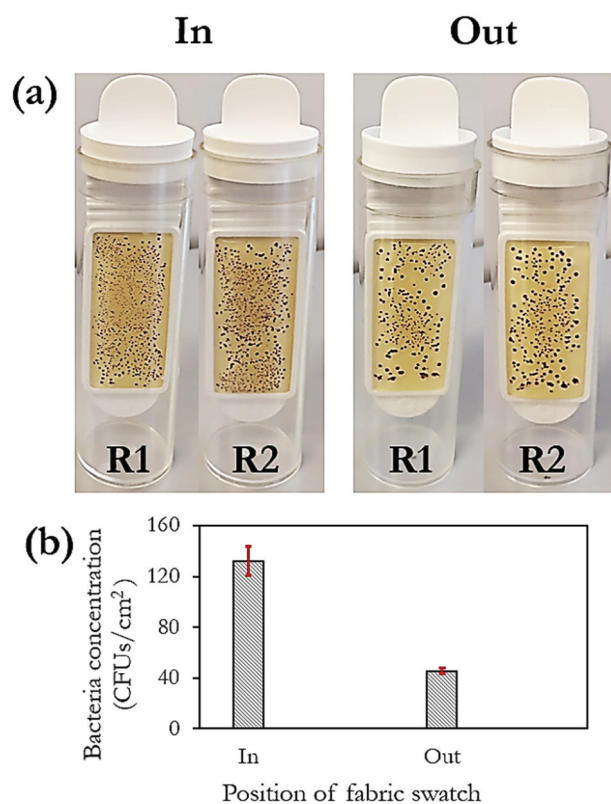


Figure 11. Disinfecting a fabric swatch attached to the middle jacket, in a scenario of 5 densely-packed jackets. The swatch was placed on the outer pocket (*Out*) and in the inner pocket (*In*), as with the penetration study. Qualitative (a) and quantitative (b) comparisons are shown for the in and out scenarios, respectively.

with the Jackets, under a dense-packing (Figure 7(c-d)). Again, this is indicative of the increased resistance to ozone entry.

As with the single garment scenario, the disinfection efficiency with multiple garments is analyzed using 5 jackets and 5 trousers. Although no evident lawns (with uncountable colonies) remain, the bacterial concentration observed when the swatch was placed in the inner pocket (Figure 11(a)) is significantly higher than that obtained with a single jacket (Figure 8(a)). Ozonating with the fabric swatch placed outside, only yields 66% bacteria removal (i.e., from 132 to 45.5 CFUs/cm²), compared to the in-pocket scenario. This demonstrates the crucial role garment spacing plays in upscaled industrial settings where there is an increased tendency to get as many garments processed in a single batch. Figure 12 illustrates a 71% difference in bacteria removal between the *In* and *Out* scenarios. Again (as with Figures 8(b) and 9(b)), the bacteria area concentration (CFUs/cm²) in Figure 12(b) (with 5 trousers) is approximately half of those obtained with 5 jackets (Figure 11(b)). Thus, garment thickness cannot be overlooked, when adequate disinfection is desired. These findings indicate

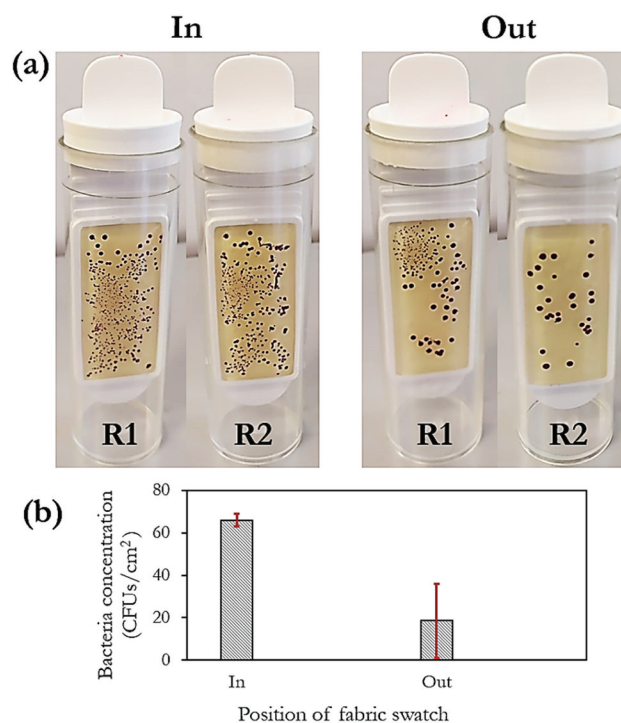


Figure 12. Disinfecting a fabric swatch attached to the middle trouser, in a scenario of 5 densely-packed trousers. The swatch was placed on the outer pocket (*Out*) and in the inner pocket (*In*), as with the penetration study. Qualitative (a) and quantitative (b) comparisons are shown for the in and out scenarios, respectively.

that a possible strategy to adopt in large-scale garment ozonation is to segregate garments according to their thicknesses and apply separate ozonation settings or to apply ozone dosages capable of effectively decontaminating the thickest garment for all other garments.

Impact of garment orientation

It is demonstrated in Figure 13 that it is best to maintain a straightened garment profile, where possible in the interest of ozone penetration and disinfection. Rather than the sharp concentration peaks observed when the sensor is left in the open (Figure 13), the in-pocket concentrations (Runs 1–4), show a more rounded profile. It is, however, shown in Figure 13(a) that the abrupt third peak gradually disappears with repeated runs of the ozonation cycle, when the trouser is folded. This further demonstrates the loosening effect, that the repeated air circulation (of the respective cycles) has on the fabric, thus yielding increased ozone penetration. The profiles of the straightened trouser scenario (Figure 13 (b)), show higher and more repeatable ozone concentrations in the pockets; thus illustrating the importance of garment hanging orientation on the attainable penetration efficiency.

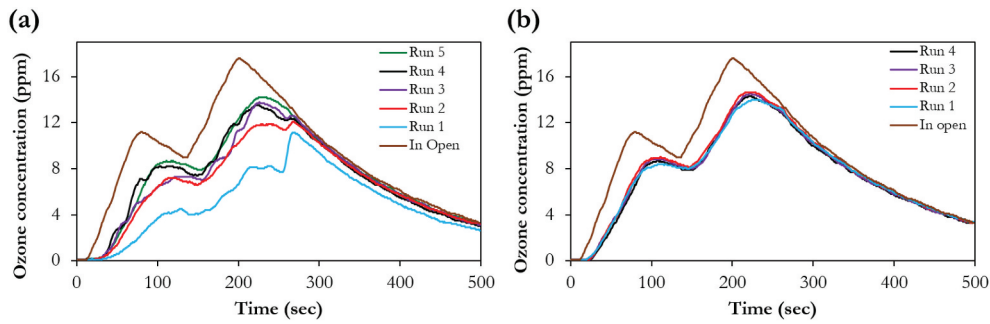


Figure 13. Ozone concentration profiles for a folded (a) and straightened (b) male trouser.

Analysis of bacterial lawn area fraction

In this scenario, 10 fabric swatches are placed on the outer and inside the inner pockets of 5 jackets in the chamber (each jacket with 2 swatches, 1 in and 1 out). This experiment aimed to evaluate the destruction of these lawns in Figure 3(e), in a densely packed condition with an increased contamination level in the chamber.

The jackets were densely packed and arranged in such a way that the swatch on the outer pocket of jacket 1 was covered by jacket 2, and the swatch on the outer pocket of jacket 2 was covered by jacket 3; with the same arrangements for jackets 3 and 4,

respectively. Thus, only the outer swatch attached to the fifth jacket was exposed directly to ozone. It is evident from Figure 14, that these conditions proved very tough for an 8-min ozonation cycle (as seen in the residual area fractions of the lawns). However, compared to the 38% lawn area fraction before ozonation (Figure 3(e)), there have been considerable reductions to as low as 5% for jacket 5. This is inevitably due to its intense exposure to ozone, given its position in the pattern. Jackets 2, 3 and 4 which occupy the central region of this arrangement, possess the highest cumulative (in and out) lawn area fractions of 30%, 25% and 29%, respectively.

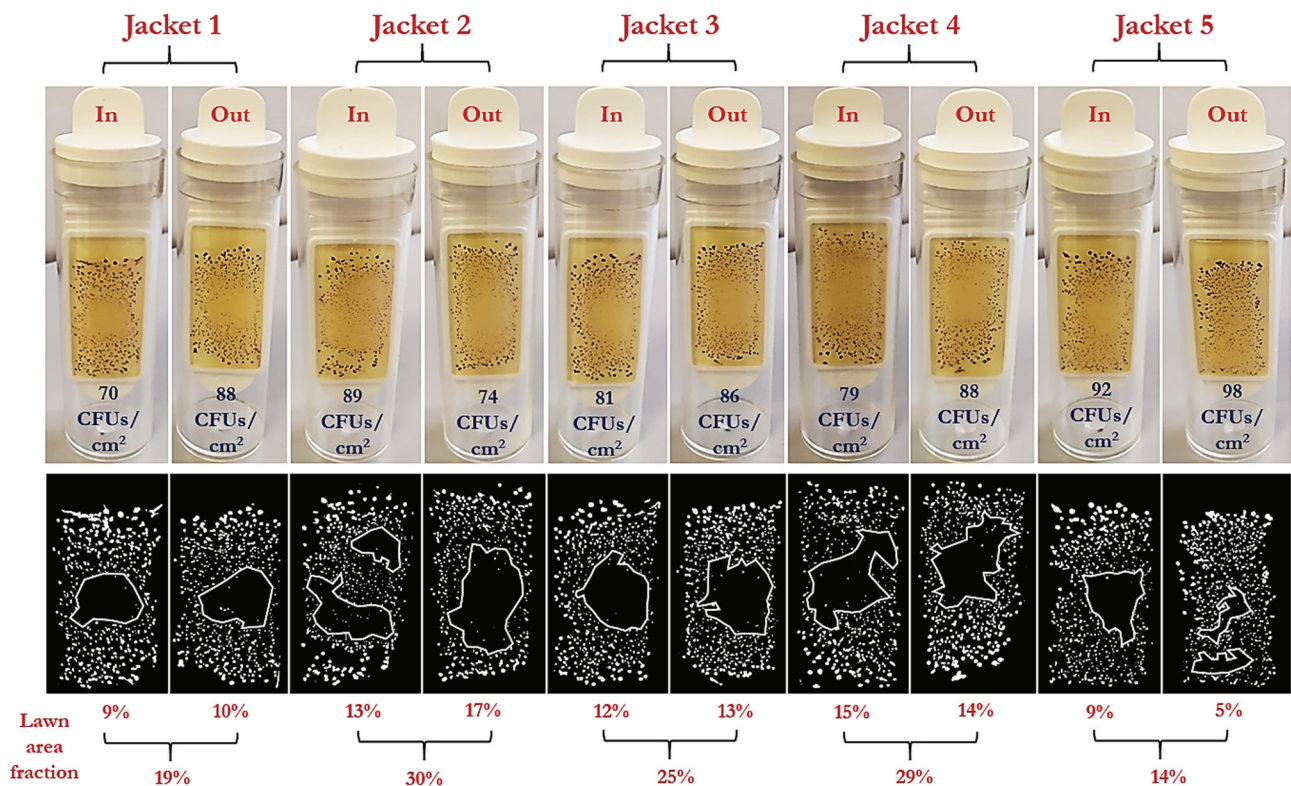


Figure 14. Analysis of bacterial lawn area for 5 densely packed jackets with 10 swatches (each jacket with 2 swatches, 1 in and 1 out). The figure shows the relative penetration of ozone influencing bacterial viability.

Effect of ozonation duration

To analyze the impact of ozonation duration, fabric swatches were placed in the inner pocket of a single jacket in the ozonation chamber. Both the lawn area fractions and the number of colonies are examined as indicators of the disinfection level. As shown in Figure 15, an ozonation duration of 4 mins leaves a significant portion of the slide covered with the bacterial lawn and is insufficient to guarantee satisfactory disinfection levels. With the application of an 8-min ozonation cycle, the lawn disappears, and the colonies become more pronounced. Relative to the bacterial concentration (CFUs/cm²) observed with the 8-min cycle, the 16- and 32-min cycles yield 97% and 99.95% bacteria removal, respectively. This is somewhat similar to the *all or none* effect reported by Broadwater et al. (1973), where a certain ozone concentration threshold is required before significant bacterial destruction is observed. In this study, an ozonation duration of 16 mins is the threshold duration for significant microbial destruction when fabric swatches are placed in the inner pockets of jackets.

It is worth mentioning that the similarity in the ozone concentration profiles (particularly the main decomposition phase, as already captured in Figure 6, facilitated

the comparison across the treatment conditions (Figure 15). However, as demonstrated in the works of Tizaoui et al. (2022) and Farooq and Tizaoui (2022), the comparability of ozone treatment conditions can be enhanced by reporting the ozone dosage – a product of concentration and time (CT value). To evaluate the differences between the ozone dosage/CT values utilized herein and in other studies, we have computed the average CT value for each treatment condition shown in Figure 15. The CT values of the 4, 8, 16 and 32 min treatment cycles are 14, 29, 57 and 83 g.min/m³. The ozone dosage of 83 g.min/m³ required for effective decontamination (Figure 15(d)) is also similar to that applied in Epelle et al. (2022b) where complete *E. coli* inactivation was observed (80 g.min/m³ corresponding to an exposure concentration of 20 ppm for 4 mins).

Analysis of fiber-bacteria interaction and inactivation via scanning electron microscopy (SEM)

In Figure 16, it can be observed that the bacteria cells tend to align with the general fiber orientation of the tested swatch (Figure 16(d,e)). Figure 16(a) shows the unaltered rod-shaped morphology of the cells before ozonation (on polished Si – wafer).

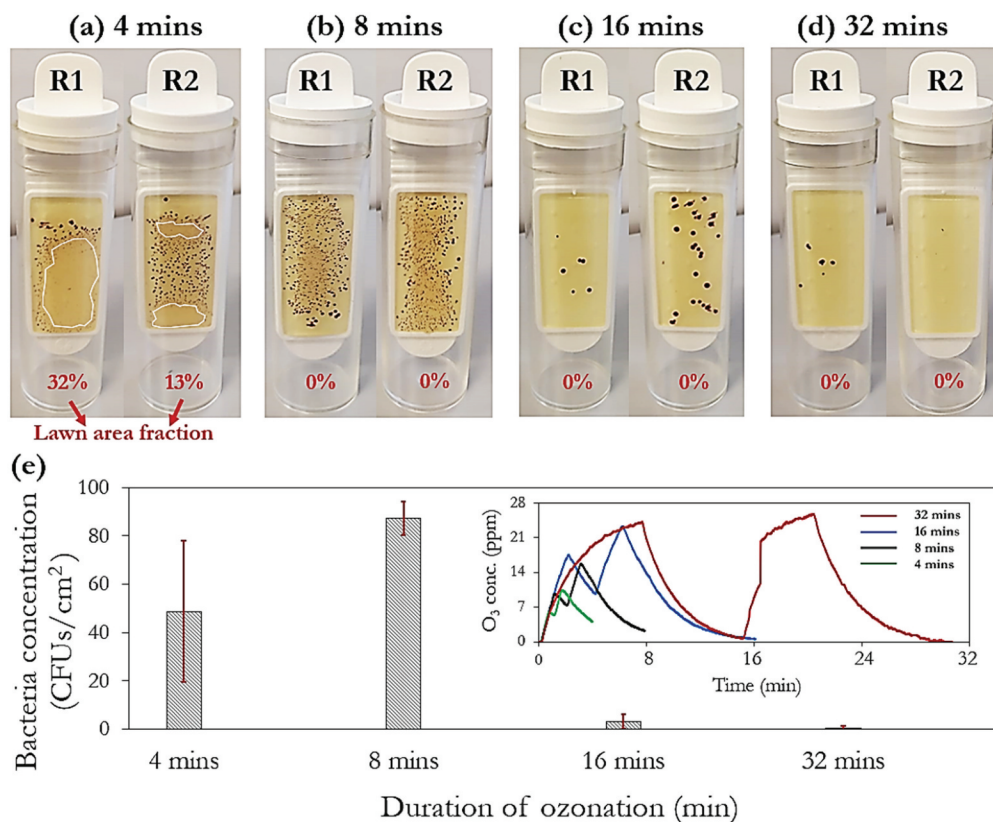


Figure 15. Impact of ozonation duration on the disinfection efficiency. Further bacterial removal is achieved with increased exposure. 4, 8, 16 and 32 min treatment cycles correspond to ozone dosages of 14, 29, 57 and 83 g.min/m³, respectively.

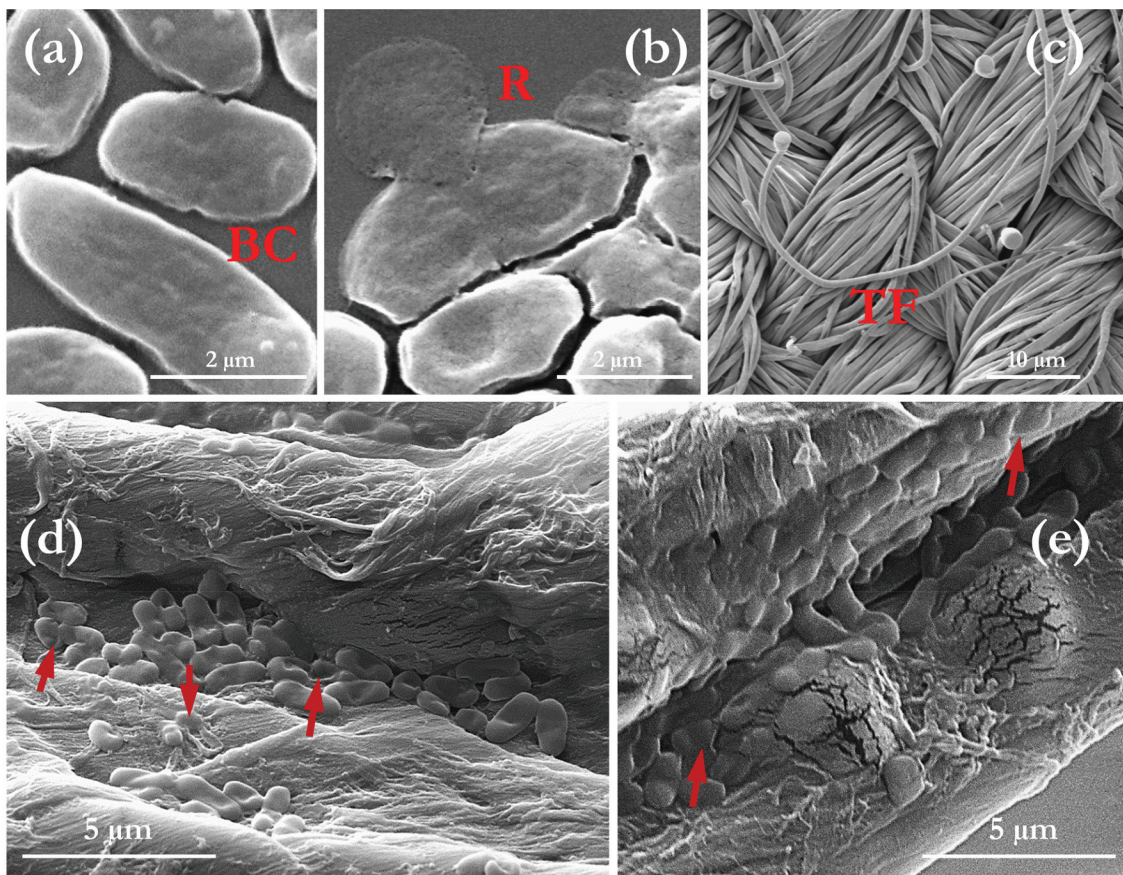


Figure 16. SEM micrographs of *E.coli* on the utilized fabric swatch before (a) and after ozonation (b); images (a) and (b) were obtained on polished Si-wafer, whereas (d, e) were imaged on the fabric swatch. TF represents textile fibers; BC, the bacterial cell; and R, the rupture/deformation of the cell membrane due to ozonation. The fabric swatch used here was obtained from the shirt samples utilised in this study.

However, in 16b, the commencement of the cell-wall disintegration can be observed; thus affecting the cell's viability and causing its eventual inactivation. It is also worth pointing out that the fibers of the swatch appear intact (without damage) in Figure 16 (c). However higher magnification image (Figure 16 (d,e)) shows some cracking in certain fiber regions. This is an indication that the adopted ozone concentrations and the corresponding exposure durations are key factors affecting the mechanical integrity of the textile material. A separate study on this effect will be worth pursuing.

Conclusions

The study has provided further insights into airborne ozone disinfection of garments under different operating conditions. The following conclusions can be derived from the results of the experiments described herein:

- The efficacy of gaseous ozone for the disinfection of textile materials contaminated with *E.coli* bacteria has been demonstrated.
- In this study, ozone dosages of 57 and 83 g.min/m³ were determined to be effective for textile treatment. This demonstrates the importance of determining the ozonation dosage threshold after which significant bacterial destruction is observed. This is particularly necessary if the gas must penetrate the hard-to-reach regions of thick garments.
- The results showed that the tightened weave structure, particularly of the female garment utilized, resulted in reduced ozone penetration (43% lower than the loosely-oriented fibers in the shirt). This demonstrates the importance of systematic garment grouping, with different cycle specifications for efficient large-scale disinfection by ozonation.
- Our results show that the mean ozone concentration reaching the armpit regions of the jacket may be reduced by 42% compared to the ozone concentration in the surrounding

chamber. Similarly, compared to a spacious arrangement of garments, densely packed garments may reduce ozone penetration by 44%. This reduction in turn affects the disinfection efficiency and should be considered when planning large-scale disinfection of textiles.

- A fully spread out pair of trousers showed a penetration level 14% higher than a folded pair of trousers. This implies that garment-hanging orientation cannot be overlooked if the desired ozone penetration and consequent disinfection are to be achieved. Large-scale disinfection operations should be planned with these considerations in mind.
- Ozone gas recirculation over our activated carbon catalyst yields a 24-times faster decomposition rate than natural ozone decomposition. This recirculation in an air-tight chamber can be utilized for small-scale ozone disinfection chambers, without the need for an external ducting system to channel excess ozone out of the environment. This rapid ozone decomposition is also beneficial from both worker safety and commercial standpoints.

A similar analysis of ozone penetration and disinfection in water for different fabric types is worthy of future investigation, particularly as more establishments are recognizing the potency of airborne ozone disinfection in the era of COVID-19.

Highlights

- Ozone penetration strongly depends on fabric thickness and morphology.
- Rapid decomposition and long ozone dwell times are competing factors.
- A rapid change in disinfection efficiency occurs between 8 and 16 mins of ozonation.
- Garment packing density severely impacts ozone penetration.

Nomenclature

CFU	Colony Forming Units
CPUR	Corrected Pick-up Rate
HMI	Human Machine Interface
TTC	2,3,5-triphenyl tetrazolium chloride

Acknowledgments

The authors gratefully acknowledge the financial support of Innovate UK (KTP 12079), as well as ACS Clothing and the University of the West of Scotland, for providing the required

equipment used in the experiments. The authors also acknowledge Mr. Kenny Richardson for his technical support in the experimental planning phase and Dr Liz Porteous for her assistance in obtaining the SEM results in this study.

Disclosure statement

No potential conflict of interest was reported by the author(s).

Notes on contributors

Emmanuel I. Epelle: Conceptualization, Methodology, Software, Data Curation, Writing Original Draft, Writing Review Draft

Andrew MacFarlane: Conceptualization, Writing Review Draft, Funding

Michael Cusack: Conceptualization, Writing Review Draft, Funding

Anthony Burns: Conceptualization, Writing Review Draft, Funding

Ngozi Amaeze: Methodology, Writing Review Draft

William Mackay: Conceptualization, Methodology, Writing Review Draft

Mohammed Yaseen: Conceptualization, Methodology, Writing Review Draft, Lead & PI.

Funding

This work was supported by the Innovate UK [KTP 12079].

References

- Batakliiev, T., V. Georgiev, M. Anachkov, S. Rakovsky, and G. E. Zaikov. 2014. "Ozone Decomposition." *Interdiscip Toxicol* 7 (2): 47–59. doi:10.2478/intox-2014-0008
- Beloti, V., M.A. Barros, J.C.D. Freitas, L.A. Nero, J.A. D. Souza, E.H. Santana, and B. Franco. 1999. "Frequency of 2, 3, 5-triphenyltetrazolium Chloride (TTC) Non-reducing Bacteria in Pasteurized Milk." *Revista de Microbiologia* 30 (2): 137–40. doi:10.1590/S0001-37141999000200009
- Broadwater, W.T., R.C. Hoehn, and P.H. King. 1973. "Sensitivity of Three Selected Bacterial Species to Ozone." *Applied Microbiology* 26 (3): 391–93. doi:10.1128/am.26.3.391-393.1973
- Dennis, R., A. Cashion, S. Emanuel, and D. Hubbard. 2020. "Ozone Gas: Scientific Justification and Practical Guidelines for Improvised Disinfection Using Consumer-Grade Ozone Generators and Plastic Storage Boxes." *The Journal of Science and Medicine* 2 (1). doi:10.37714/josam.v2i1.35.
- Dosti, B., Z. Guzel-Seydim, and A.K. Greene. 2005. "Effectiveness of Ozone, Heat and Chlorine for Destroying Common Food Spoilage Bacteria in Synthetic Media and Biofilms." *International Journal of Dairy Technology* 58 (1): 19–24. doi:10.1111/j.1471-0307.2005.00176.x

- Epelle, E.I., A. Macfarlane, M. Cusack, A. Burns, N. Amaeze, K. Richardson, W. Mackay, M.E. Rateb, and M. Yaseen. 2022a. "Stabilisation of Ozone in Water for Microbial Disinfection." *Environments* 9(4): 45. 1–19. doi:10.3390/environments9040045.
- Epelle, E.I., A. Macfarlane, M. Cusack, A. Burns, B. Thissera, W. Mackay, M.E. Rateb, and M. Yaseen. 2022b. "Bacterial and Fungal Disinfection via Ozonation in Air." *Journal of Microbiological Methods* 194:106431. doi: 10.1016/j.mimet.2022.106431.
- Farooq, S., and C. Tizaoui. 2022. "A Critical Review on the Inactivation of Surface and Airborne SARS-CoV-2 Virus by Ozone Gas." *Critical Reviews in Environmental Science and Technology* 1–23. doi: 10.1080/10643389.2022.2043094.
- Gonçalves, A.A., and G.A. Gagnon. 2011. "Ozone Application in Recirculating Aquaculture System: An Overview." *Ozone: Science & Engineering* 33 (5): 345–67. doi:10.1080/01919512.2011.604595
- Guzel-Seydim, Z.B., A.K. Greene, and A.C. Seydim. 2004. "Use of Ozone in the Food Industry." *LWT-Food Science and Technology* 37 (4): 453–60. doi:10.1016/j.lwt.2003.10.014
- Karim, N., S. Afroj, K. Lloyd, L.C. Oaten, D.V. Andreeva, C. Carr, A.D. Farmery, I.D. Kim, and K.S. Novoselov. 2020. "Sustainable Personal Protective Clothing for Healthcare Applications: A Review." *ACS Nano* 14 (10): 12313–40. doi:10.1021/acsnano.0c05537
- Kim, J.G., A.E. Yousef, and S. Dave. 1999. "Application of Ozone for Enhancing the Microbiological Safety and Quality of Foods: A Review." *Journal of Food Protection* 62 (9): 1071–87. doi:10.4315/0362-028X-62.9.1071
- Körlü, A. 2018. "Use of Ozone in the Textile Industry." *Textile Industry and Environment* 1–23. doi:10.5772/intechopen.81774.
- Kowalski, W.J., W.P. Bahnfleth, B.A. Striebig, and T. S. Whittam. 2003. "Demonstration of a Hermetic Airborne Ozone Disinfection System: Studies on E. Coli." *AIHA Journal* 64 (2): 222–27. doi:10.1080/15428110308984811
- Lage Filho, F.A. 2010. "Ozone Application in Water Sources: Effects of Operational Parameters and Water Quality Variables on Ozone Residual Profiles and Decay Rates." *Brazilian Journal of Chemical Engineering* 27 (4): 545–54. doi:10.1590/S0104-66322010000400006
- Li, W., 1998. Kinetics and Mechanism of Ozone Decomposition and Oxidation of Ethanol on Manganese Oxide Catalysts. Doctoral dissertation, Virginia Polytechnic Institute and State University.
- Malik, S.N., P.C. Ghosh, A.N. Vaidya, and S.N. Mudliar. 2020. "Hybrid Ozonation Process for Industrial Wastewater Treatment: Principles and Applications: A Review." *Journal of Water Process Engineering* 35:101193. doi: 10.1016/j.jwpe.2020.101193.
- Manjunath, S.N., M. Sakar, M. Katapadi, and R. G. Balakrishna. 2021. "Recent Case Studies on the Use of Ozone to Combat Coronavirus: Problems and Perspectives." *Environmental Technology & Innovation* 21:101313. doi: 10.1016/j.eti.2020.101313.
- Martinelli, M., F. Giovannangeli, S. Rotunno, C.M. Trombetta, and E. Montomoli. 2017. "Water and Air Ozone Treatment as an Alternative Sanitizing Technology." *Journal of Preventive Medicine and Hygiene* 58 (1): E48.
- Neral, B. 2018. "Quality of the Household Ozone Laundering." *Industria Textila* 69 (4): 304–09. doi:10.35530/IT.069.04.1454
- Rekhate, C.V., and J.K. Srivastava. 2020. "Recent Advances in Ozone-based Advanced Oxidation Processes for Treatment of wastewater-A Review." *Chemical Engineering Journal Advances* 100031. <https://doi.org/10.1016/j.cej.2020.100031>
- Rice, R.G., M. DeBrum, D. Cardis, and C. Tapp. 2009. "The Ozone Laundry Handbook: A Comprehensive Guide for the Proper Application of Ozone in the Commercial Laundry Industry." *Ozone: Science & Engineering* 31 (5): 339–47. doi:10.1080/01919510903091318
- Rogers, W.J. 2012. "Sterilisation Techniques for Polymers." In *Sterilisation of Biomaterials and Medical Devices*. 151–211. Woodhead Publishing.
- Rosenblum, J., C. Ge, Z. Bohrerova, A. Yousef, and J. Lee. 2012. "Ozonation as a Clean Technology for Fresh Produce Industry and Environment: Sanitizer Efficiency and Wastewater Quality." *Journal of Applied Microbiology* 113 (4): 837–45. doi:10.1111/j.1365-2672.2012.05393.x
- Rubio-Romero, J.C., M. Del Carmen Pardo-ferreira, J. A. Torrecilla-García, and S. Calero-Castro. 2020. "Disposable Masks: Disinfection and Sterilization for Reuse, and Non-certified Manufacturing, in the Face of Shortages during the COVID-19 Pandemic." *Safety Science* 129:104830. doi: 10.1016/j.ssci.2020.104830.
- Sevimli, M.F., and H.Z. Sarikaya. 2002. "Ozone Treatment of Textile Effluents and Dyes: Effect of Applied Ozone Dose, pH and Dye Concentration." *Journal of Chemical Technology & Biotechnology: International Research in Process, Environmental & Clean Technology* 77 (7): 842–50. doi:10.1002/jctb.644
- Sharrer, M.J., and S.T. Summerfelt. 2007. "Ozonation Followed by Ultraviolet Irradiation Provides Effective Bacteria Inactivation in a Freshwater Recirculating System." *Aquacultural Engineering* 37 (2): 180–91. doi:10.1016/j.aquaeng.2007.05.001
- Summerfelt, S.T. 2003. "Ozonation and UV Irradiation—an Introduction and Examples of Current Applications." *Aquacultural Engineering* 28 (1–2): 21–36. doi:10.1016/S0144-8609(02)00069-9
- Summerfelt, S.T., M.J. Sharrer, S.M. Tsukuda, and M. Gearheart. 2009. "Process Requirements for Achieving Full-flow Disinfection of Recirculating Water Using Ozonation and UV Irradiation." *Aquacultural Engineering* 40 (1): 17–27. doi:10.1016/j.aquaeng.2008.10.002
- Szeto, W., W.C. Yam, H. Huang, and D.Y. Leung. 2020. "The Efficacy of Vacuum-ultraviolet Light Disinfection of Some Common Environmental Pathogens." *BMC Infectious Diseases* 20 (1): 1–9. doi:10.1186/s12879-020-4847-9
- Tizaoui, C., R. Stanton, E. Statkute, A. Rubina, E. Lester-Card, A. Lewis, P. Holliman, and D. Worsley. 2022. "Ozone for SARS-CoV-2 Inactivation on Surfaces and in Liquid Cell Culture Media." *Journal of Hazardous Materials* 428:128251. doi: 10.1016/j.jhazmat.2022.128251.
- Valdenassi, L., M. Franzini, G. Ricevuti, L. Rinaldi, A.C. Galoforo, and U. Tirelli. 2020. "Potential Mechanisms by Which the Oxygen-ozone (O₂-O₃) Therapy Could Contribute to the Treatment against the Coronavirus COVID-19." *European Review for Medical and Pharmacological Sciences* 24 (8): 4059–61. doi:10.26355/eurrev_202004_20976
- Wang, J., X. Quan, S. Chen, H. Yu, and G. Liu. 2019. "Enhanced Catalytic Ozonation by Highly Dispersed CeO₂ on Carbon Nanotubes for Mineralization of Organic Pollutants." *Journal of Hazardous Materials* 368:621–29. doi: 10.1016/j.jhazmat.2019.01.095.